RSC Advances

PAPER

View Article Online
View Journal | View Issue

Cite this: *RSC Adv.*, 2022, **12**, 1228

Improvement of cytotoxicity and necrosis activity of ganoderic acid a through the development of PMBN-A.Her2-GA as a targeted nano system

P. Motamed Fath, *[a] M. Rahimnejad,[bc] S. Moradi-kalbolandi,[d] B. Ebrahimi Hosseinzadeh[a] and T. Jamshidnejad-tosaramandani[e]

Received 28th August 2021
Accepted 11th December 2021

DOI: 10.1039/d1ra06488f

rsc.li/rsc-advances

The targeting nano carriers have been promptly proposed to overcome the current obstacles in conventional chemotherapy approaches for cancer. Currently, PMBN (poly[MPC-*co*-(BMA)-*co*-(MEONP)]), is considered as a promising amphiphilic polymer that could be easily targeted and conjugated to hydrophobic substances with low bioavailability. To target breast cancer cells overexpressing human epidermal receptor 2 (HER2) receptors, anti-HER2 monoclonal antibody (A.Her2) was conjugated to PMBN and afterward loaded with ganoderic acid A (GA-A) as an anti-cancer metabolite. The efficacy of conjugation and loading was reasonably favourable. The rod shape of the polymer with a size of approximately 160 ± 30 nm was confirmed. Our results indicated that PMBN-A.Her2-GA is an anionic nanostructure with an appropriate form and capable of being applied in cancer therapy. Subsequently, cytotoxicity analysis revealed an improved anti-proliferative effect of GA-A.

1. Introduction

Cancer is considered one of the world's leading causes of death.[1] Recent reports estimate the total global cost associated with cancer therapy to be a hundred billion US$.[2] Due to the growing side effects of conventional chemotherapeutic approaches, there is more attention to finding alternative ways for improving the immune system to target the advanced stages of tumors.[3] Several natural herbal components have been conventionally applied to treat various disorders for a long time. Current investigations have been focused on natural extracts of fungi, particularly those with low cellular toxicity for normal tissues. It should be noted that not only efficacy but also the cost-effectiveness of any investigation for a new therapeutic approach should be considered in cancer therapy to determine the cancer-related health care cost. *Ganoderma lucidum* (*G. lucidum*), normally raised as Lingzhi in China, is a fungal material that has been applied extensively in Asian nations for routine treatments.[4] Its pharmacological properties include immune-modulating, anti-inflammatory, anti-cancer, anti-diabetic, anti-oxidative, radical-scavenging, and anti-aging effects.[5–7] *G. lucidum*, contains more than 90% water, carbohydrate, crude fat, fibre, and protein[8]. Moreover, it consists of diverse bioactive components such as terpenoids, steroids, phenols, glycoproteins, and polysaccharides.[9] It has been reported that triterpenes and polysaccharides are the main physiologically active ingredients of *G. lucidum*.[10] The growth of cell lines such as the human prostate PC-3 and bladder cancers has been reported to be inhibited following the exposure to the *G. lucidum* extract.[11–13] Furthermore, ganoderic acid inhibits cell proliferation and induced apoptosis in the human colon and breast carcinoma cell lines.[14–21]

Breast cancer is one of the most common cancers in the world. Recently, targeted therapy with antibodies or in combination with nano carriers has been regarded as a novel therapeutic approach to specifically target tumour markers.[22] Trastuzumab (Herceptin) is the first recombinant human-specific IgG1 monoclonal antibody applied in HER2 overexpressed breast cancer patients.[23] HER2 is a tyrosine kinase from the family of epidermal growth factor receptors or EGFRs[24] involved in various signalling pathways and considered promising targets in breast cancer therapeutic approaches.[25] HER2 plays a vital role in controlling growth, survival, and cell differentiation.[26] Recombinant mAbs such as Trastuzumab and Pertuzumab are commercially approved for targeting Her2 in breast cancer therapy.[27,28] Despite all advantages in the clinic, frequent mutations and subsequent monoclonal antibody

[a]*Faculty of New Sciences and Technologies, University of Tehran, Tehran, Iran. E-mail: puria.motamed@yahoo.com; Tel: +98-919-4500 621*
[b]*Biomedical Engineering Institute, School of Medicine, Université de Montréal, Montreal, Canada*
[c]*Research Centre, Centre Hospitalier de L'Université de Montréal (CRCHUM), Montréal, Canada*
[d]*Recombinant Proteins Department, Breast Cancer Research Center, Motamed Cancer Institute, ACECR, Tehran, Iran*
[e]*Nano Biotechnology Department, Faculty of Innovative Science and Technology, Razi University, Kermanshah, Iran*

resistance through activation of alternative pathways might occur.[27,29,30] Hence, there is a crucial need for improved clinical efficiency of anti-Her2 mAb. Targeted therapy with nanotechnology as drug delivery has been considered a promising approach.[31,32] Following this technology, the drug dose and toxicity in healthy tissues will be reduced, whereas anti-tumour efficacy will be enhanced.[33–35] In drug delivery systems (DDSs), biopolymers or biocompatible polymers have been extensively applied.[36–40] 2-Methacryloyloxyethyl phosphorylcholine (MPC) polymer is a biocompatible polymer with the same polar group (phosphorylcholine group) as biomembranes and thus lacks any protein absorption.[41] MPC polymers have been applied as surface modifiers in numerous medical apparatus to develop biocompatibility.[42] The MPC polymers are extremely hydrophilic due to their *n*-butyl methacrylate units; therefore, copolymers such as MPC could be water-soluble. As a result, hydrophobic monomer units might be involved in the solubilisation of hydrophobic agents and improve their water solubility and bioavailability.[43] Due to the incorporation of hydrophobic substances by MPC, the possibility of their application as a carrier for non-soluble substances in aqueous media has been investigated.[41,44] Poly[MPC-*co*-(BMA)-*co*-(MEONP)] (PMBN) is a part of MPC polymer with active ester groups capable of being conjugated to various proteins under moderate physiological conditions.[45] PMBN might be a promising tool for targeted therapy through proper ligands or antibody conjugation. In the current study, growth inhibition and antitumor characteristics of GA-A in combination with anti-Her2 mAb-conjugated PMBN (PMBN-A.Her2-GA) on HER2 overexpressed SKBR3 cell lines in comparison to Her2 negative MCF7 cell lines were investigated. Briefly, PMBN as an amphiphilic and targetable polymer was conjugated with anti-Her2 mAb and loaded with GA-A to target Her2 overexpressed breast cancer cell lines directly and deliver GA-A as a fungal anti-tumor agent (Fig. 1).

2. Materials and methods

2.1. Materials

RPMI 1640 cell culture and Fetal Bovine Saline (FBS) were provided from Sigma-Aldrich Co., Germany. Amicon filter was procured from Merck Millipore Co., USA, ganoderic acid A from BOC Science Co., USA, and anti-HER2 mAb Trastuzumab (Herceptin®) was purchased from Aryogen Pharmed (Karaj, Iran).

3. Methods

3.1. Targetable amphiphilic nano polymer, PMBN

PMBN polymer has been developed in our previous study with the composition of 40 mol% MPC, 50 mol% BMA, and 10 mol% of MEONP.[46] The structure of the polymer was confirmed by Fourier transform infrared spectroscopy (FT-IR MB102, BOMEM Inc., Switzerland) using the KBr pellet technique. Proton nuclear magnetic resonance device (H-NMR DRX 300, Bruker Avance Co., USA) was applied by $CDCI_3$ as solvent and tetramethylsilane (TMS) as standard internal material. Moreover, dynamic light scattering measurement (DLS, Nano-ZS, Malvern Co., UK) was applied to calculate the size of nanoparticles (NPs), size distribution, and zeta potential of the NPs' surface. Subsequently, a scanning electron microscope (SEM VEGA II, Tescan Co., Czech Republic) and transmission electron

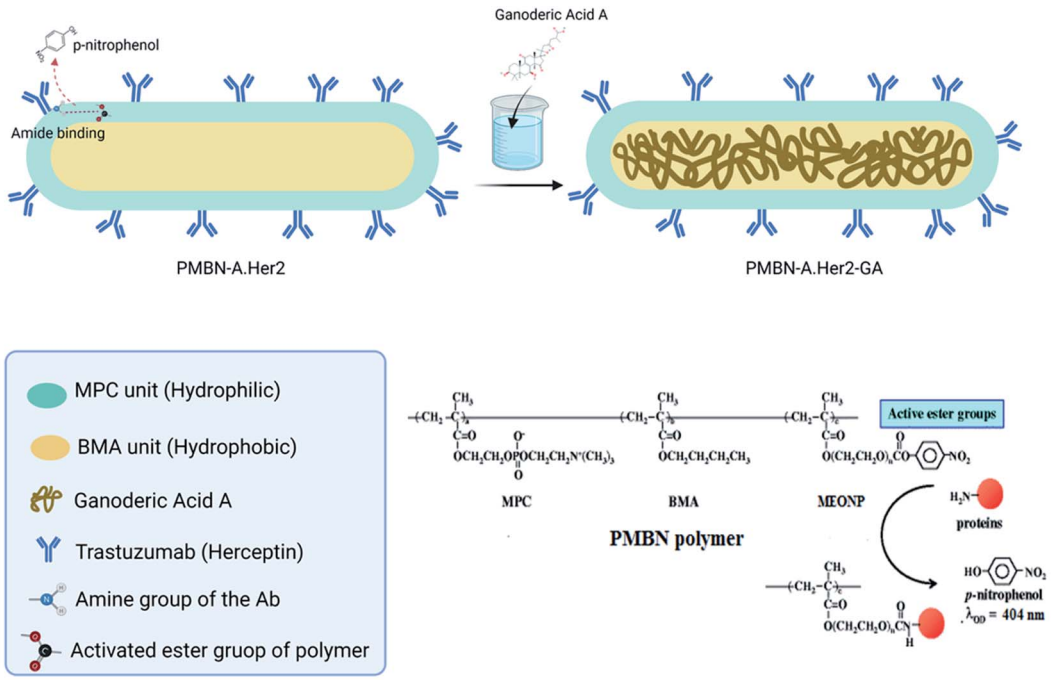

Fig. 1 The conjugation of PMBN to anti-Her2 mAb, loaded with GA-A, a fungal anti-tumour agent. Anti-Her2 mAbs are conjugated to MPC units as hydrophilic units and GA-A is attached to the BMA units due to its hydrophobicity.

microscope imaging system (TEM EM10C-80 KV, Zeiss Co., Germany) evaluated the shape and size of the developed NPs.

3.2. Conjugation of PMBN-antiHer2mAb

2 mg of polymer with 30 μl concentration of Trastuzumab (Herceptin®) Aryogen Pharmed (Karaj, Iran) was added to PBS at pH ~7.4, and thoroughly mixed at 4 °C for 48 h. Afterward, the obtained mixture was centrifuged (rpm: 5000 g, time: 13 min) using a 30 KDa Amicon falcon filter (Amicon® Ultra-15 device, Merck Millipore Ltd, USA) to remove unbound antibodies and *p*-nitrophenol groups. The efficiency of filtration was checked *via* absorption spectroscopy at 280 and 404 nm for anti-Her2 mAb and *p*-nitrophenol, respectively, *via* a UV-Vis spectrophotometer (Nanodrop 2000C, Thermo Scientific Co, USA). In that case, anti-her2 mAb would make an amide binding with the active ester group of MEONP monomer through the free $-NH_2$ group, and *p*-nitrophenol will be released. To determine the amide binding and efficiency, the following solutions were prepared:

(1) 1 mg of PMBN in 1 ml of NaOH (0.2 mol ml^{-1}), (2) 1 mg of PMBN in 1 ml of water, and (3) 1 mg of PMBN-A.Her2 in 1 ml of water. The absorbance of each solution was measured at 404 nm to evaluate the efficiency of conjugation by a spectrophotometer, and the amide binding was analysed by FT-IR measurement.

3.3. Incorporation of conjugated PMBN-antiHer2mAb with GA-A

The dissolved GA-A (1 ml) in ethanol was added to PMBN-A.Her2-GA conjugates and mixed gently at room temperature. Amicon falcon filtered the solution, and the loading efficiency was analysed through the absorbance measurement at 255 nm. The size and zeta potential of PMBN-A.Her2-GA were determined by DLS, and also the structure and size of the nano system were investigated by field emission scanning electron microscope (FESEM MIRA3, Tescan Co., Czech Republic) with a magnification of 700 000.

3.4. Functional activity of conjugated PMBN-A.Her2-GA

3.4.1. Cytotoxicity. The functional activity of our developed nano system on SKBR3 cells (HER2 over-expressing breast cancer cell line) was evaluated in comparison to the MCF7 cell line as the negative control. Briefly, the SKBR3 and MCF7 cells (University of Tehran, Tehran, Iran) were (5×10^3 cells per well) seeded into 96-well plates and incubated for 24 h. Next, free GA-A, PMBN-GA, and our developed PMBN-A.Her2-GA was suspended within the 10% v/v serum added, and the cells were incubated at 37 °C. Cell viability was investigated through cell staining (dead cells in red and live cells in green) (Life Technologies, USA) following days 1 and 7 using 1 μM calcein AM and 2 μM ethidium homodimer-3 in culture medium stained cells, which were observed under fluorescent microscopy (Leica DM IRB).

3.4.2. Metabolic activity of cells. Metabolic activity (cells proliferation) was evaluated using the Alamar Blue assay (Resazurin Cell Viability Assay Kit, Biotium, USA) following days 1 and 7. In brief, 10% v/v resazurin solution was added to each sample mentioned above and incubated at 37 °C for 3 h. Then, 100 μl of supernatant of incubated samples was transferred to a 96-well plate, and fluorescence emission intensity was quantified using a micro-plate fluorescence reader (λ_{ex} 560 nm, λ_{em} 590 nm, BioTek Instruments Inc., Synergy 4, USA).

3.4.3. Cell apoptosis analysis. SKBR3 and MCF7 cell lines were cultured in RPMI medium supplemented with 10% fetal bovine serum at 37 °C. Briefly, cells were seeded at 10^6 cells per ml to 96-well plates with 10% FBS containing 5% CO_2 and incubated overnight at 37 °C. The next day, free GA-A, PMBN-GA-A, and our developed PMBN-A.Her2-GA were added to each well. After 24 and 48 h of incubation, the apoptosis rate of cells in response to cognate treatment was analyzed using Annexin V Apoptosis Detection Kit (KeyGEN Biotech Co., Ltd, Nanjing, China) according to the instruction. Subsequently, the cells were analyzed by FACS caliber (FACScan, BD Biosciences, Franklin Lakes, NJ, USA) programmed with CellQuest software (BD Biosciences, Franklin Lakes, NJ, USA).

3.4.4. Statistical analysis. Statistical analysis was performed using GraphPad Prism 5 software. One-way ANOVA and Tukey's multiple comparison tests were used to compare multiple groups. $P < 0.05$ was considered to be statistically significant. All experiments were performed at least in triplicate.

4. Results and discussions

4.1. Characterization of PMBN polymer

First, the polymer was analysed by FT-IR and H-NMR methods. The specific peak at 1727 cm^{-1} was related to the carbonyl group, the peak at 1086 cm^{-1} was for ($-POCH_2-$), and the 964 cm^{-1} for ($N^+(CH_3)_3$) group. Furthermore, the MPC monomer peaks at 1.81 ppm for (CH_3-C), at 4–4.3 ppm for ($N+CCH_2-$, $POCH_2C$, $-OCH_2CH_2OP-$), and at 3.5 ppm for ($N+CH_3$) were determined by H-NMR analysis. BMA block peaks were at 1.0 ppm for (CH_3-C), at ~4 ppm for ($O(CH_2)_3-C$), and at 1.3 ppm for ($C-CH_3$). Finally, the MEONP monomer was confirmed by peaks at ~0.8 ppm for (CH_3-C), 3.1 ppm for (OCH_2CH_2O), and 7.0 and 8.1 ppm for protons of the aromatic ring. All the desired structures of the polymer were as expected as confirmed. In the next step, the size and zeta potential of the polymer were

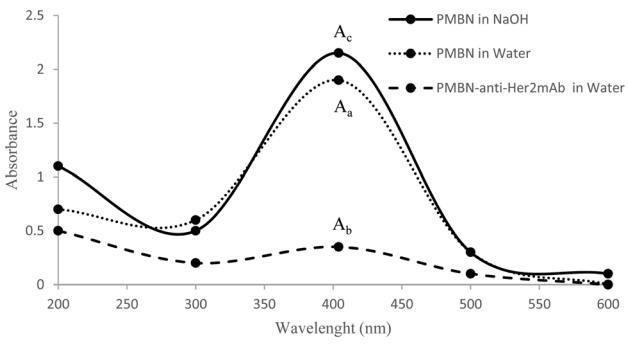

Fig. 2 The absorbance of free *p*-nitrophenol in three different solutions, Aa, Ab, and Ac, to measure the efficiency of the PMBN-anti-Her2mAb conjugate.

analyzed by DLS. The analysis revealed −8.7 mV for the surface charge, which indicates an anionic polymer. Following conjugation and incorporation, the enhanced or reduced values should be measured to evaluate the quality of the constructed nano system. Moreover, the size of 52.18 nm and the Poly Disparity Index (PDI) of 0.11 confirmed the polymer as a nano polymer with "monodisperse" characteristics. The size and structure of the polymer were checked with SEM and TEM microscopy. Results indicate the dimensions of 40 nm for polymer. The variance between DLS, SEM, and TEM data was probably due to the larger hydrodynamic diameter in DLS analysis, which was typically larger than the diameters determined by SEM and TEM microscopy as a capping agent. The synthesized polymer was notably rod-shaped. Rouslahti *et al.* reported that in contrast to spherical NPs, rod-shaped NPs (nano rods) show high endothelial preference in both *in vitro* and *in vivo*.[47] Furthermore, such particles seem to be superior for targeting in tumor xenografts.[48] Thus, this type of structure might be a promising candidate to design an appropriate nano carrier for DDS.[39,40]

4.2. Conjugation of polymer and mAb

After the conjugation of the polymer with anti-Her2 mAb, the solution was filtered. The absorbance of flow-through was measured at 280 and 404 nm to evaluate any unbound antibody and *p*-nitrophenol, respectively, which confirmed the accuracy of our filtration step. The results confirmed that no free *p*-nitrophenol or anti-Her2 in the solution that could interfere with subsequent studies or possibly have toxic effects were found (not shown). To measure the efficiency of conjugation, three solutions were prepared, as mentioned before. The polymer in NaOH solution, leading to the total release of the *p*-nitrophenol group, can be considered as a reference value. However, due to hydrolysis, fewer groups will be released from the polymer in water. Consequently, the remaining *p*-nitrophenol after conjugation will be released following the hydrolysis. After the absorbance measurement at 404 nm (specific for free *p*-nitrophenol) according to Fig. 1, and by the calculation 1 below, the efficacy of conjugation was calculated to be 72.1% and confirmed (Fig. 2).

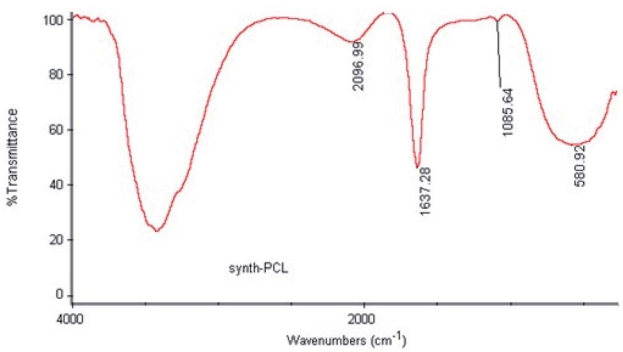

Fig. 3 FT-IR analysis showed a specific amide-binding peak at 1637 cm^{-1} and confirmed the interaction of the MEONP monomer with anti-Her2mAb.

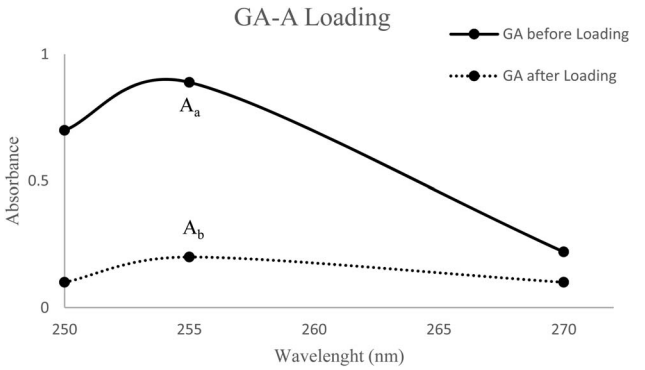

Fig. 4 Evaluation of GA-A incorporation into conjugated NPs. The absorbance of conjugated NPs before and subsequent GA-A loading was measured at 255 nm, as shown, and the reduced absorbance confirmed the accuracy of incorporation.

Table 1 Comparison of size, zeta potential, and PDI of NPs before and after incorporation with GA-A

	PMBN	PMBN-A.Her2-GA
Size	52.18 nm	279.8 nm
Zeta potential	−8.47 mV	−43.8 mV
PDI	0.116	0.436

$$\frac{Aa - Ab}{Ac} \times 100 = \frac{1.9 - 0.35}{2.15} \times 100 = 72.1\% \quad (1)$$

In addition, the FT-IR analysis of conjugation showed a peak at 1637 cm^{-1}, which is specific for amide binding and indicates the interaction between active ester groups of MEONP monomer and free $-NH_2$ of anti-Her2mAb (Fig. 3). Hence, it can be concluded that the polymer can be conjugated with any biomolecules with free $-NH_2$, and it is considered a potential candidate to target desired cancerous cells.

4.3. GA-A loading to PMBN-anti Her2 mAb conjugate

To investigate the efficiency of incorporation, the concentration of GA-A in the solution of PMBN-A.Her2 was analyzed at 255 nm in comparison to GA-A before incorporation. As shown in Fig. 4,

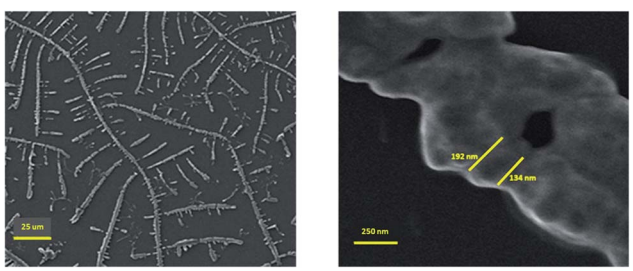

Fig. 5 The results of the FESEM microscopy. The rod-shaped structure of the constructed PMBN-A.Her2-GA confirmed the intact polymer conformation subsequent to conjugation and loading. The left and the right magnification is 1k× and 100k×, respectively, and confirmed the rod-shaped structure with the size of 160 ± 30 nm.

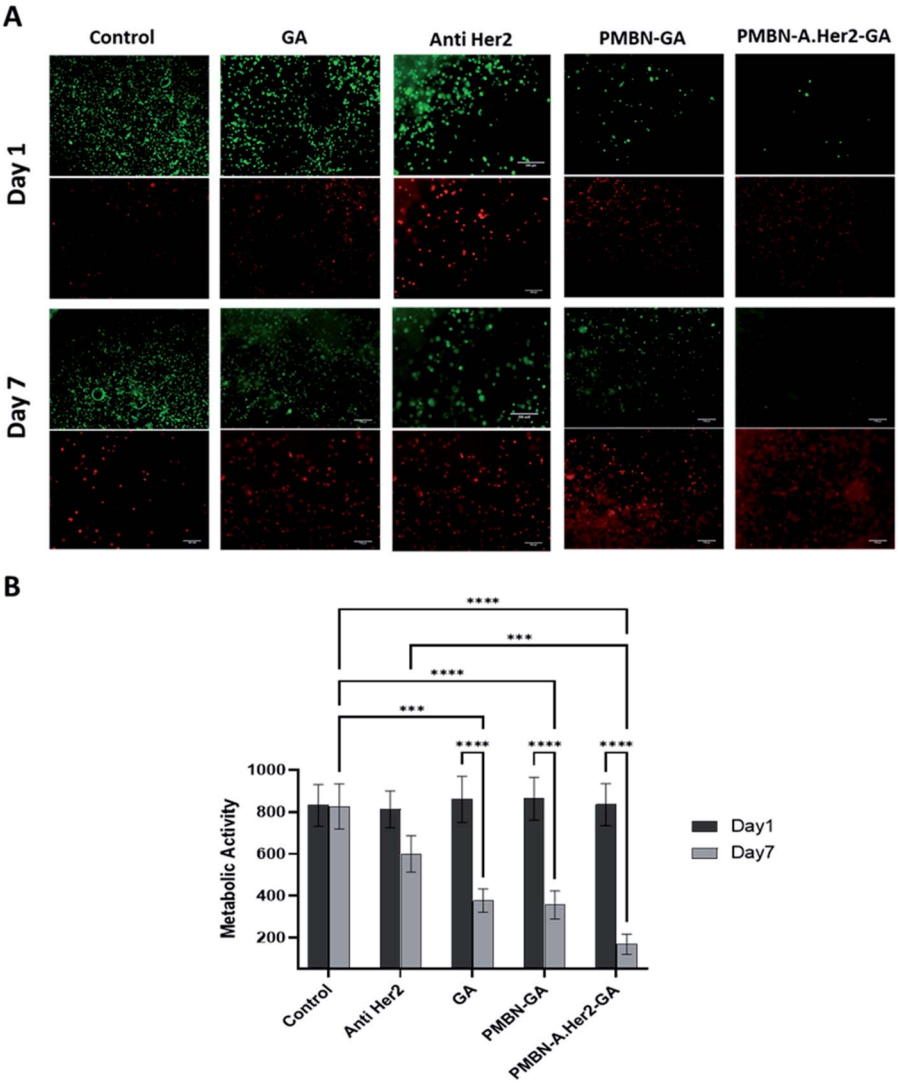

Fig. 6 Cytotoxicity analysis of nano system. (A) Cell viability *via* fluorescent microscopic images. Following days 1 and 7 under 4 different conditions as shown in the figure. Dead and live cells stained in red and green, respectively (Life Technologies, USA), subsequent to the addition of 1 μM calcein AM and 2 μM ethidium homodimer-3 in the culture medium. (B) Alamar Blue assay, the metabolic activity of cells evaluated at days 1 and 7 (Resazurin Cell Viability Assay Kit, Biotium, USA) (Mean ± SD), (ns: not significant, ***$p < 0.001$, ****$p < 0.0001$).

and through the following eqn (2), the efficacy of loading was approximately 77.5%. According to this result, GA-A as a hydrophobic agent with less than 1% water solubility, became soluble in combination with the amphiphilic polymer. As a result, this polymer might be applied as an appropriate candidate for incorporating hydrophobic drugs or agents.[49,50]

$$\frac{(\mathrm{Aa}-\mathrm{Ab})}{\mathrm{Aa}} \times 100 = \frac{(0.89-0.20)}{0.89} \times 100 = 77.5\ \% \qquad (2)$$

4.4. Characterization of synthesized nano system, PMBN-A.Her2-GA

The synthesized nano system was analyzed by DLS. The specifications of this nano carrier were compared with PMBN, as depicted in Table 1. Following the conjugation and loading, results obtained from the FESEM microscope indicate the enhanced size of the polymer from 52 nm to 280 nm. Furthermore, the PDI was still under 0.5, which is acceptable for a nano system. It should be noted that not only does the polymer remain anionic, but also the zeta potential (ZP) increased, remarkably. Due to electrostatic interactions, more cellular uptake of nanoparticles (NPs) with ZP-43 mV compared to NPs with lower ZP or with positive ZP has been demonstrated in various studies.[51] Generally, cellular absorption of these particles is because of (1) non-specific absorption of NPs on cell membrane (2) formation of NPs cluster. Limbach *et al.* found that the human lung fibroblast cells rapidly absorb NPs with negative ZP.[52] The absorption of negative NPs on the positive sites of the cell membrane by electrostatic interactions leads to neutralization and subsequently makes the plasma membrane induce the endocytosis phenomena.[53] It has been demonstrated

that aggregation of NP with negative surface charge and approximate size of 150 nm at the tumor sites is superior. These results prompted us to develop nano carriers for pharmaceutical applications with improved therapeutic effects.[54] Comparison of two positive and negative NPs with the same values of ZP demonstrated the preference of phagocytosis systems to cationic particles regardless of their constructions.[55] In another investigation, a comparison of cerium oxide NPs with positive and negative surface charges confirmed the high tendency of protein absorption with the positive ones,[51] which could be an excellent challenge for DDSs.

On the other hand, the zeta potential is a critical factor for the stability of NPs solutions. Due to the repulsive forces, the high surface electrical charge of NPs leads to no agglomeration in buffer solutions.[56,57] According to the theory of DLVO, the stability of solutions and colloids results from the balance between attraction and repulsion of van der walls forces of surface net charges. If the ZP value is below the specific amount,

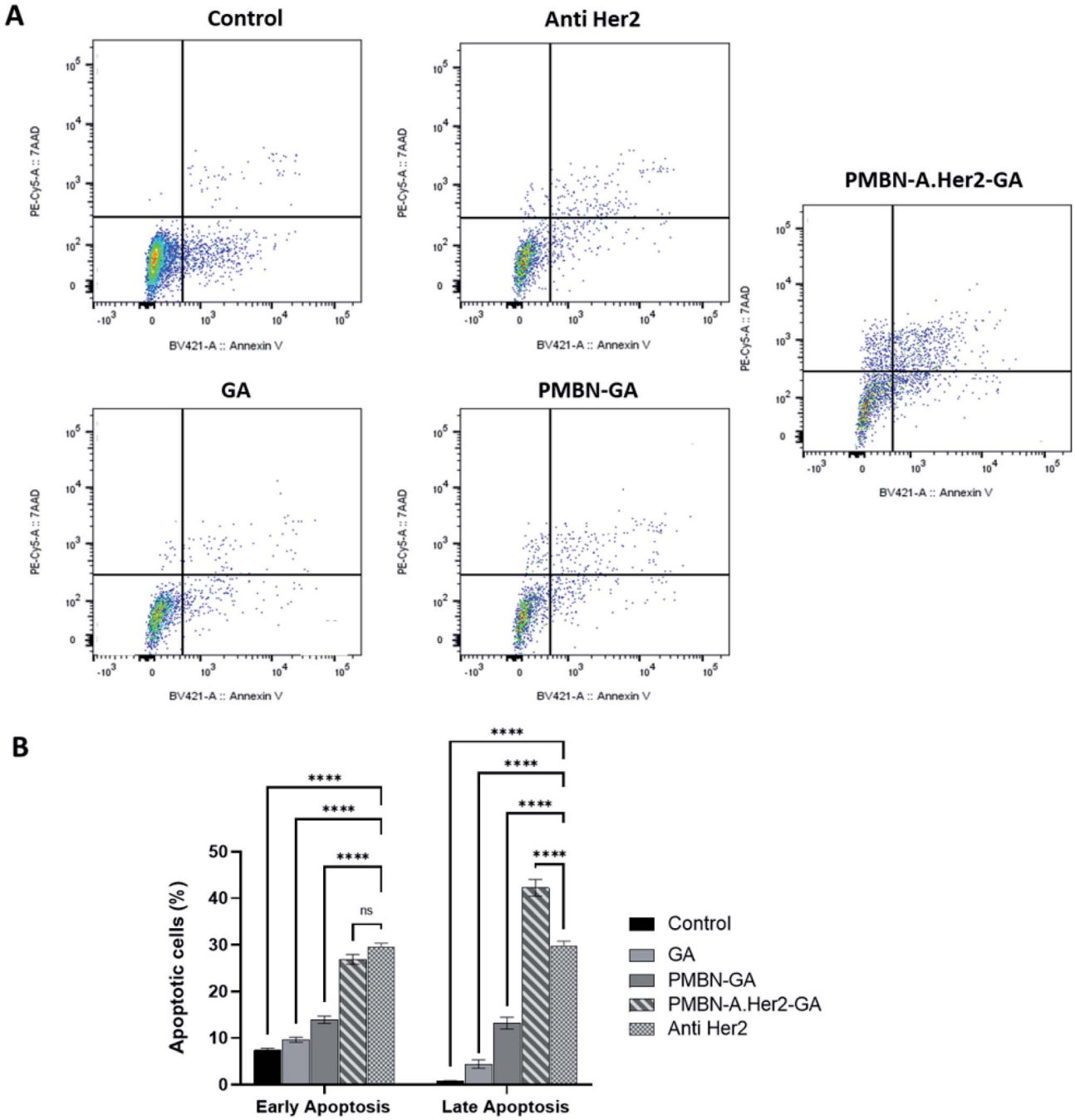

Fig. 7 Cell apoptosis assay. (A) Raw data obtained from flow cytometry of SKBR3 cell line under GA-A, PMBN-GA, and PMBN-A.Her2-GA treatments in comparison to control (MCF7 treated with PMBN-A.Her2-GA). (B) Early and late apoptosis rate of cells (mean ± SD), (****p < 0.0001). As depicted in the figure, PMBN-A.Her2-GA leads to enhanced apoptosis compared to others.

the particles tend to be agglomerated. In contrast, for ZP above ±30 mv, the system tends to be stable.[58,59] The ZP is an important physicochemical parameter for the stability of nano solutions, and the minimum acceptable ZP value for static and electrostatic stability is ±20 mv.

Furthermore, the results of FESEM microscopy are shown in Fig. 5. The rod-shaped structure of the nano system confirmed the intact polymer conformation subsequent to conjugation and loading. As mentioned before, rod-shaped structures are more effective and successful than other nano structures.[47,48] In addition, the size of the targeted nano system was approximately 160 ± 30 nm, which is a desirable size for a nano system in drug delivery applications. Our result is consistent with DLS analysis (the difference relates to hydrodynamic diameter, as mentioned).

4.5. Cytotoxicity analysis of the nano system

According to IC_{50} of PMBN-A.Her2-GA compared to GA-A solution as shown in Fig. 6, it was concluded that targeting the polymer with anti-Her2mAb leads to enhanced cytotoxicity of the fungal metabolite up to 75%. Reduced IC_{50} of PMBN-A.Her2-GA compared to each agent at SKBR3 as positive cell line was more intuitive than MCF7 as negative cell line due to potent targeted DDS. Furthermore, to evaluate the role of targeting, the efficiency of PMBN-A.Her2-GA and PMBN-GA-A were compared to other studies.[30,60] No improvement in toxicity of PMBN-GA was shown compared to the targeted nano system. Two crucial factors for improved toxicity of the conjugate system include: (1) enhanced solubility and bioavailability of hydrophobic GA-A metabolite, following its incorporation in PMBN. (2) Specific targeting of desired cells after the conjugation of anti-Her2mAb with PMBN. In another study by Motamed *et al.*, the toxicity of GA-A was reported to be similar to Paclitaxel (PTX) as a conventional chemotherapeutic drug.[61]

The cytotoxicity assays of PMBN and PMBN-A.Her2-GA (Fig. 6 and 7) indicate no toxicity effect of unconjugated PMBN on both cell lines, consistent with previous studies,[50] and confirmed the biocompatibility of polymer and nano systems. In addition, our results indicate that anti-Her2 monoclonal antibody (A.Her2) plays an inhibitory role in the proliferation of $Her2^+$ cells. Cancer cell (SKBR3) death is shown in the cell line treated with anti Her2 (Trastuzumab) and decreased metabolic activity and cancer cell proliferation at day 7, but in less extent in comparison with cell line treated with PMBN-A.Her2-GA. Previous studies also showed an increase in the efficiency of Trastuzumab when combined with anti-tumor drugs.[62,63] Similarly, PMBN-A.Her2-GA and PMBN-GA demonstrate higher SKBR3 cell apoptosis than Anti Her2, GA, and control groups, as shown in Fig. 7. In particular, PMBN-A.Her2-GA shows ~30 and 40% early and late apoptosis, respectively, indicating higher cancer cell killing efficiency of the nano system than other groups.

One of the limitations in this study is that other toxicities such as reproductive toxicity are essential to investigate. However, GA-A is inherently not toxic since this compound has been a natural material used in Asian countries for many years. In combination with the PMBN nano carrier, to date, no reproductive toxicity has been reported for GA-A. Motamed *et al.* reported that PMBN is not toxic individually, and there are no side effects.[46] Ishihara *et al.* also noted that this polymer is biocompatible with potential bioapplications.[50]

5. Conclusion

In our study, the amphiphilic PMBN was conjugated with anti-Her2mAb to directly target HER2+ breast cancer cell line, and anti-tumoral fungal metabolite GA-A was incorporated with this targeted nano DDS for the first time. Following characterization, the rod-shaped structure with an approximate size of 160 ± 30 nm and anionic zeta potential of −43.8 mv was confirmed. The toxicity of PMBN-A.Her2-GA was studied on positive and negative cell lines, which showed more than 50% improved toxicity compared to GA-A. Overall, our developed nano system might be considered a promising candidate for an alternative to conventional chemotherapeutic approaches. In a similar work by Gharbavi *et al.*, a similar system based on PMBN polymer loaded with Paclitaxel agent was used for drug delivery, and in *vitro* drug release, blood biocompatibility, as well as the cytotoxicity and apoptosis were analyzed that cleared great features of this nano polymer.[64]

In this regard, further investigation in the animal model of tumors is essential and remains the goal of our future work. The system's stability, like a stress stability test, must be performed to figure out the lifetime of the designed system for further works.

Conflict of interest

The authors declare no conflict of interest in this study.

Acknowledgements

There is no financial support for this research. Fig. 1 was prepared using http://www.biorender.com.

References

1 C. Mattiuzzi and G. Lippi, Current cancer epidemiology, *J Epidemiol Glob Health.*, 2019, **9**(4), 217.
2 J. Cortes, J. M. Perez-García, A. Llombart-Cussac, G. Curigliano, N. S. El Saghir, F. Cardoso, *et al.* Enhancing global access to cancer medicines, *CA: Cancer J. Clin.*, 2020, **70**(2), 105–124.
3 S. Poorhosseini, M. Hashemi, O. N. Alipour, A. Izadi, E. Moslemi, Z. Ravesh, *et al.* New Gene Profiling in Determination of Breast Cancer Recurrence and Prognosis in Iranian Women, *Asian Pac J Cancer Prev*, 2015, **17**, 155–160.
4 Q. Liu and L. Tie. *Preventive and therapeutic effect of Ganoderma (Lingzhi) on diabetes*. Ganoderma and Health. 2019, pp. 201–15.
5 N. Laçin, S. B. İzol, F. İpek and M. C. Tuncer, Ganoderma lucidum, a promising agent possessing antioxidant and anti-inflammatory effects for treating calvarial defects with

graft application in rats1, *Acta Cir. Bras.*, 2019, **34**(9), e201900904.

6 P. Rossi, R. Difrancia, V. Quagliariello, E. Savino, P. Tralongo, C. L. Randazzo, *et al.* B-glucans from Grifola frondosa and Ganoderma lucidum in breast cancer: an example of complementary and integrative medicine, *Oncotarget*, 2018, **9**(37), 24837.

7 D. Sohretoglu and S. Huang, Ganoderma lucidum polysaccharides as an anti-cancer agent, *Anti-Cancer Agents Med. Chem.*, 2018, **18**(5), 667–674.

8 S. Sudheer, I. Alzorqi, A. Ali, P. G. Cheng, Y. Siddiqui and S. Manickam, Determination of the biological efficiency and antioxidant potential of Lingzhi or Reishi medicinal mushroom, Ganoderma lucidum (Agaricomycetes), cultivated using different agro-wastes in Malaysia, *Int. J. Med. Mushrooms*, 2018, **20**(1), 89–100.

9 A. Bhardwaj and K. Misra. Therapeutic medicinal mushroom (Ganoderma lucidum): A review of bioactive compounds and their applications. *Plant-and Marine-Based Phytochemicals for Human Health*. 2018:pp. 191–242.

10 Y. Yang, H. Zhang, J. Zuo, X. Gong, F. Yi, W. Zhu, *et al.* Advances in research on the active constituents and physiological effects of Ganoderma lucidum, *Biomed. Dermatol.*, 2019, **3**(1), 1–17.

11 X. Wang, B. Wang, L. Zhou, X. Wang, V. P. Veeraraghavan, S. K. Mohan, *et al.* Ganoderma lucidum put forth anti-tumor activity against PC-3 prostate cancer cells *via* inhibition of Jak-1/STAT-3 activity, *Saudi J. Biol. Sci.*, 2020, **27**(10), 2632–2637.

12 X. Wang, G. Fang and Y. Pang, Chinese medicines in the treatment of prostate cancer: From formulas to extracts and compounds, *Nutrients*, 2018, **10**(3), 283.

13 J. Yuen, D. Mak, E. Chan, M. Gohel and C. Ng, Tumor inhibitory effects of intravesical Ganoderma lucidum instillation in the syngeneic orthotopic MB49/C57 bladder cancer mice model, *J. Ethnopharmacol.*, 2018, **223**, 113–121.

14 J. Jiang, V. Slivova, K. Harvey, T. Valachovicova and D. Sliva, Ganoderma lucidum suppresses growth of breast cancer cells through the inhibition of Akt/NF-κB signaling, *Nutr. Cancer*, 2004, **49**(2), 209–216.

15 H. Hu, N. S. Ahn, X. Yang, Y. S. Lee and K. S. Kang, Ganoderma lucidum extract induces cell cycle arrest and apoptosis in MCF-7 human breast cancer cell, *Int. J. Cancer*, 2002, **102**(3), 250–253.

16 C. I. Müller, T. Kumagai, J. O'Kelly, N. P. Seeram, D. Heber and H. P. Koeffler, Ganoderma lucidum causes apoptosis in leukemia, lymphoma and multiple myeloma cells, *Leuk. Res.*, 2006, **30**(7), 841–848.

17 D. Elumalai, T. Suman, M. Hemavathi, C. Swetha, R. Kavitha, C. Arulvasu, *et al.* Biofabrication of gold nanoparticles using Ganoderma lucidum and their cytotoxicity against human colon cancer cell line (HT-29), *Bull. Mater. Sci.*, 2021, **44**(2), 1–6.

18 K. Na, K. Li, T. Sang, K. Wu, Y. Wang and X. Wang, Anticarcinogenic effects of water extract of sporoderm-broken spores of Ganoderma lucidum on colorectal cancer *in vitro* and *in vivo*, *Int. J. Oncol.*, 2017, **50**(5), 1541–1554.

19 X. Ji, Q. Peng and M. Wang, Anti-colon-cancer effects of polysaccharides: A mini-review of the mechanisms, *Int. J. Biol. Macromol.*, 2018, **114**, 1127–1133.

20 A. Barbieri, V. Quagliariello, V. Del Vecchio, M. Falco, A. Luciano, N. J. Amruthraj, *et al.* Anticancer and anti-inflammatory properties of Ganoderma lucidum extract effects on melanoma and triple-negative breast cancer treatment, *Nutrients*, 2017, **9**(3), 210.

21 Y. Zhang, Ganoderma lucidum (Reishi) suppresses proliferation and migration of breast cancer cells *via* inhibiting Wnt/β-catenin signaling, *Biochem. Biophys. Res. Commun.*, 2017, **488**(4), 679–684.

22 K. Barzaman, J. Karami, Z. Zarei, A. Hosseinzadeh, M. H. Kazemi, S. Moradi-Kalbolandi, *et al.* Breast cancer: Biology, biomarkers, and treatments, *Int. Immunopharmacol.*, 2020, **84**, 106535.

23 J. Molnar *Analysis of Organotropic Metastasis in Relation to Herceptin Response of HER2 Positive Breast Cancer Cells*, California State University, Northridge; 2017.

24 C. A. Russell, Personalized medicine for breast cancer: it is a new day!, *Am. J. Surg.*, 2014, **207**(3), 321–325.

25 R. Butti, S. Das, V. P. Gunasekaran, A. S. Yadav, D. Kumar and G. C. Kundu, Receptor tyrosine kinases (RTKs) in breast cancer: signaling, therapeutic implications and challenges, *Mol. Cancer*, 2018, **17**(1), 1–18.

26 K. Araki and Y. Miyoshi, Mechanism of resistance to endocrine therapy in breast cancer: the important role of PI3K/Akt/mTOR in estrogen receptor-positive, HER2-negative breast cancer, *Breast Cancer*, 2018, **25**(4), 392–401.

27 S. Moradi-Kalbolandi, A. Hosseinzade, M. Salehi, P. Merikhian and L. Farahmand, Monoclonal antibody-based therapeutics, targeting the epidermal growth factor receptor family: from herceptin to Pan HER, *J. Pharm. Pharmacol.*, 2018, **70**(7), 841–854.

28 S. Yu, J. Zhang, Y. Yan, X. Yao, L. Fang and H. Xiong, A novel asymmetrical anti-HER2/CD3 bispecific antibody exhibits potent cytotoxicity for HER2-positive tumor cells, *J. Exp. Clin. Cancer Res.*, 2019, **38**(1), 1–16.

29 A. Elamir, S. Ajith, N. Al Sawaftah, W. Abuwatfa, D. Mukhopadhyay and V. Paul, Ultrasound-triggered herceptin liposomes for breast cancer therapy, *Sci. Rep.*, 2021, **11**(1), 7545.

30 H. H. Oberg, C. Kellner, D. Gonnermann, S. Sebens, D. Bauerschlag and M. Gramatzki, Tribody [(HER2) 2xCD16] is more effective than trastuzumab in enhancing γδ T cell and natural killer cell cytotoxicity against HER2-expressing cancer cells, *Front. Immunol.*, 2018, **9**, 814.

31 S. K. Singh, S. Singh, J. W. Licard Jr and R. Singh, Drug delivery approaches for breast cancer, *Int. J. Nanomed.*, 2017, **12**, 6205.

32 Y. Yan, X. Cheng, L. Li, R. Zhang, Y. Zhu and Z. Wu, A Novel Small Molecular Antibody, HER2-Nanobody, Inhibits Tumor Proliferation in HER2-Positive Breast Cancer Cells *In Vitro* and *In Vivo*, *Front. Oncol.*, 2021, **11**, 1724.

33 B. Kim, J. Shin, J. Wu, D. T. Omstead, T. Kiziltepe, L. E. Littlepage, *et al.* Engineering peptide-targeted liposomal nanoparticles optimized for improved selectivity

for HER2-positive breast cancer cells to achieve enhanced *in vivo* efficacy, *J. Controlled Release*, 2020, **322**, 530–541.

34 R. K. Dhritlahre and A. Saneja, Recent advances in HER2-targeted delivery for cancer therapy, *Drug Discovery Today*, 2021, **5**, 1319–1329.

35 G. Rinnerthaler, S. P. Gampenrieder and R. Greil, HER2 directed antibody-drug-conjugates beyond T-DM1 in breast cancer, *Int. J. Mol. Sci.*, 2019, **20**(5), 1115.

36 H. Danafar, A. Sharafi, H. Kheiri Manjili and S. Andalib, *Sulforaphane delivery using mPEG–PCL co-polymer nanoparticles to breast cancer cells*, Pharmaceutical development and technology, 2016, pp. 1–10.

37 H. K. Manjili, A. Sharafi, H. Danafar, M. Hosseini, A. Ramazani and M. H. Ghasemi, Poly(caprolactone)–poly(ethylene glycol)–poly(caprolactone)(PCL–PEG–PCL) nanoparticles: a valuable and efficient system for *in vitro* and *in vivo* delivery of curcumin, *RSC Adv.*, 2016, **6**(17), 14403–14415.

38 S. Al-MGA Awi, H. Naderi-Manesh, Z. Mohammad Hassan, H. Yeganeh, S. Nikzad and H. Kheiri Manjili, Construction of Polyurethane Polymeric-based Nano-carriers for Curcumin in Cancer Therapy, *Modares Med. Sci.: Pathobiol.*, 2014, **17**(4), 25–39.

39 H. Danafar, H. Manjili and M. Najafi, Study of Copolymer Composition on Drug Loading Efficiency of Enalapril in Polymersomes and Cytotoxicity of Drug Loaded Nanoparticles, *Drug Res.*, 2016, **66**(09), 495–504.

40 X. Fang, J. Cao and A. Shen, Advances in anti-breast cancer drugs and the application of nano-drug delivery systems in breast cancer therapy, *J. Drug Delivery Sci. Technol.*, 2020, **57**, 101662.

41 K. Ishihara, M. Mu and T. Konno, Water-soluble and amphiphilic phospholipid copolymers having 2-methacryloyloxyethyl phosphorylcholine units for the solubilization of bioactive compounds, *J. Biomater. Sci., Polym. Ed.*, 2018, **29**(7–9), 844–862.

42 Y. Liu, M. C. Munisso, A. Mahara, Y. Kambe and T. Yamaoka, Anti-platelet adhesion and *in situ* capture of circulating endothelial progenitor cells on ePTFE surface modified with poly(2-methacryloyloxyethyl phosphorylcholine) (PMPC) and hemocompatible peptide 1 (HCP-1), *Colloids Surf., B.*, 2020, **193**, 111113.

43 K. Ishihara, Revolutionary advances in 2-methacryloyloxyethyl phosphorylcholine polymers as biomaterials, *J. Biomed. Mater. Res., Part A*, 2019, **107**(5), 933–943.

44 K. Yoshie, S. Yada, S. Ando and K. Ishihara, Effects of inner polarity and viscosity of amphiphilic phospholipid polymer aggregates on the solubility enhancement of poorly water-soluble drugs, *Colloids Surf., B*, 2020, **195**, 111215.

45 T. Konno, J. Watanabe and K. Ishihara, Conjugation of enzymes on polymer nanoparticles covered with phosphorylcholine groups, *Biomacromolecules*, 2004, **5**(2), 342–347.

46 P. Motamed Fath, F. Yazdian, R. Jamjah, B. Ebrahimi Hosseinzadeh, M. Rahimnezhad, R. Sahraeian, *et al.* Synthesis and Characterization of PMBN, As a Biocompatible Nano Polymer for Bio-Applications, *Cell J.*, 2017, **19**(2), 269–277.

47 P. Kolhar, A. C. Anselmo, V. Gupta, K. Pant, B. Prabhakarpandian, E. Ruoslahti, *et al.* Using shape effects to target antibody-coated nanoparticles to lung and brain endothelium, *Proc. Natl. Acad. Sci.*, 2013, **110**(26), 10753–10758.

48 K. S. Chu, W. Hasan, S. Rawal, M. D. Walsh, E. M. Enlow, J. C. Luft, *et al.* Plasma, tumor and tissue pharmacokinetics of Docetaxel delivered *via* nanoparticles of different sizes and shapes in mice bearing SKOV-3 human ovarian carcinoma xenograft, *Nanomed.: Nanotechnol. Biol. Med.*, 2013, **9**(5), 686–693.

49 T. Shimada, M. Ueda, H. Jinno, N. Chiba, M. Wada, J. Watanabe, *et al.* Development of targeted therapy with paclitaxel incorporated into EGF-conjugated nanoparticles, *Anticancer Res.*, 2009, **29**(4), 1009–1014.

50 N. Chiba, M. Ueda, T. Shimada, H. Jinno, J. Watanabe, K. Ishihara, *et al.* Novel immunosuppressant agents targeting activated lymphocytes by biocompatible MPC polymer conjugated with interleukin-2, *Eur. Surg. Res.*, 2007, **39**(2), 103–110.

51 S. Patil, A. Sandberg, E. Heckert, W. Self and S. Seal, Protein adsorption and cellular uptake of cerium oxide nanoparticles as a function of zeta potential, *Biomaterials*, 2007, **28**(31), 4600–4607.

52 L. K. Limbach, Y. Li, R. N. Grass, T. J. Brunner, M. A. Hintermann, M. Muller, *et al.* Oxide nanoparticle uptake in human lung fibroblasts: effects of particle size, agglomeration, and diffusion at low concentrations, *Environ. Sci. Technol.*, 2005, **39**(23), 9370–9376.

53 S. Honary and F. Zahir, Effect of zeta potential on the properties of nano-drug delivery systems-a review (Part 1), *Trop. J. Pharm. Res.*, 2013, **12**(2), 255–264.

54 C. He, Y. Hu, L. Yin, C. Tang and C. Yin, Effects of particle size and surface charge on cellular uptake and biodistribution of polymeric nanoparticles, *Biomaterials*, 2010, **31**(13), 3657–3666.

55 S. Honary and F. Zahir, Effect of zeta potential on the properties of nano-drug delivery systems-a review (Part 2), *Trop. J. Pharm. Res.*, 2013, **12**(2), 265–273.

56 U. Kedar, P. Phutane, S. Shidhaye and V. Kadam, Advances in polymeric micelles for drug delivery and tumor targeting, *Nanomed.: Nanotechnol. Biol. Med.*, 2010, **6**(6), 714–729.

57 K. K. Sawant and S. S. Dodiya, Recent advances and patents on solid lipid nanoparticles, *Recent Pat. Drug Delivery Formulation*, 2008, **2**(2), 120–135.

58 A. Prokop, E. Kozlov, G. Carlesso and J. M. Davidson. Hydrogel-based colloidal polymeric system for protein and drug delivery: physical and chemical characterization, permeability control and applications. *Filled Elastomers Drug Delivery Systems*: Springer; 2002. pp. 119–73.

59 M. Beck-Broichsitter, C. Ruppert, T. Schmehl, A. Guenther, T. Betz, U. Bakowsky, *et al.* Biophysical investigation of pulmonary surfactant surface properties upon contact with

polymeric nanoparticles *in vitro*, *Nanomed.: Nanotechnol. Biol. Med.*, 2011, **7**(3), 341–350.

60 J. O. Eloy, R. Petrilli, D. L. Chesca, F. P. Saggioro, R. J. Lee, J. M. Marchetti, *et al.* Anti-HER2 immunoliposomes for co-delivery of paclitaxel and rapamycin for breast cancer therapy, *Eur. J. Pharm. Biopharm.*, 2017, **115**, 159–167.

61 F. Alambin, P. M. Fath, B. E. Hosseinzadeh, A. H. Zarmi, R. Sahraeian and F. Yazdian, Leukemia stem cells, direct targeting of CD123 based on the nano-smart polymer PMBN, *RSC Adv.*, 2016, **6**(98), 96138–96146.

62 Y. Fujimoto, T. Y. Morita, A. Ohashi, H. Haeno, Y. Hakozaki and M. Fujii, Combination treatment with a PI3K/Akt/mTOR pathway inhibitor overcomes resistance to anti-HER2 therapy in PIK3CA-mutant HER2-positive breast cancer cells, *Sci. Rep.*, 2020, **10**(1), 21762.

63 S. Pernas and S. M. Tolaney, HER2-positive breast cancer: new therapeutic frontiers and overcoming resistance, *Ther. Adv. Med. Oncol.*, 2019, **11**, 1758835919833519.

64 M. Gharbavi, A. Sharafi, P. Motamed Fath, S. Oruji, H. Pakzad and H. Kheiri Manjili, Formulation and Biocompatibility of Microemulsion-Based PMBN as an Efficient System for Paclitaxel Delivery, *J. Appl. Biotechnol. Rep.*, 2021, **8**(1), 51–62.